AD-A166 275 MEAN TRAJECTORY GAUSSIAN WAVE PACKET APPROACH TO ROTATIONALLY INELASTIC M..(U) CALIFORNIA UNIV SANTA BARBARA QUANTUM INST B JACKSON ET AL. FEB 86 TR-10 1/1

UNCLASSIFIED N00014-81-K-0598 F/G 20/10 NL

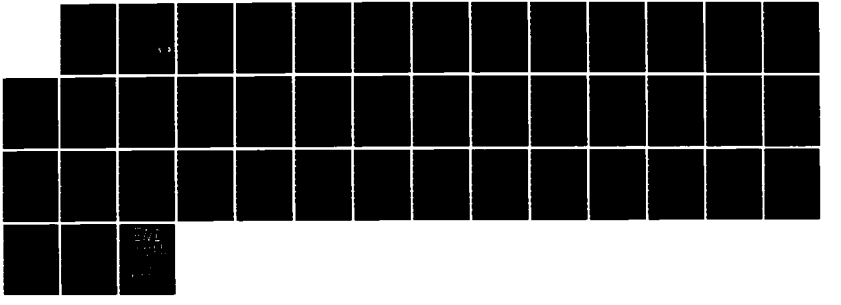

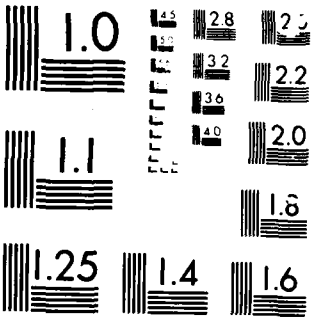

MICROCOPY RESOLUTION TEST CHART

AD-A166 275

(12)

REPORT DOCUMENTATION PAGE

READ INSTRUCTIONS BEFORE COMPLETING FORM

1. REPORT NUMBER: 10	2. GOVT ACCESSION NO.
3. RECIPIENT'S CATALOG NUMBER	
4. TITLE (and Subtitle): MEAN TRAJECTORY GAUSSIAN WAVE PACKET APPROACH TO ROTATIONALLY INELASTIC MOLECULE-SURFACE DIFFRACTION	5. TYPE OF REPORT & PERIOD COVERED: Annual Technical Report
	6. PERFORMING ORG. REPORT NUMBER
7. AUTHOR(s): Bret Jackson and Horia Metiu	8. CONTRACT OR GRANT NUMBER(s): N00014-81-K-0598
9. PERFORMING ORGANIZATION NAME AND ADDRESS: University of California, Quantum Institute, Santa Barbara, CA 93106	10. PROGRAM ELEMENT, PROJECT, TASK AREA & WORK UNIT NUMBERS: NR 056-766/4-21-81 (472)
11. CONTROLLING OFFICE NAME AND ADDRESS: Office of Naval Research, Department of the Navy, Code: 612A: DKB, Arlington, VA 22217	12. REPORT DATE: February 1986
	13. NUMBER OF PAGES: 37
14. MONITORING AGENCY NAME & ADDRESS(if different from Controlling Office): Office of Naval Research Detachment Pasadena, 1030 East Green Street, Pasadena, CA 91105	15. SECURITY CLASS. (of this report): unclassified/unlimited
	15a. DECLASSIFICATION/DOWNGRADING SCHEDULE

16. DISTRIBUTION STATEMENT (of this Report)

Approved for public release; distribution unlimited

17. DISTRIBUTION STATEMENT (of the abstract entered in Block 20, if different from Report)

This document has been approved for public release and sale; its distribution is unlimited.

18. SUPPLEMENTARY NOTES

Accepted: J. Chem. Phys.

DTIC ELECTE APR 0 4 1986 S D

19. KEY WORDS (Continue on reverse side if necessary and identify by block number)

rotationally inelastic molecule-surface diffraction

20. ABSTRACT (Continue on reverse side if necessary and identify by block number)

The rotationally inelastic diffraction of H_2 from a corrugated surface is investigated using a mean trajectory model. The center of mass motion is treated using Gaussian wave packets, which propagate on a rotationally averaged potential. This trajectory in turn drives the rotational transitions. The method is non-perturbative and allows for changes in m_j, the rotational orientation, and agress well with recent close coupling calculations. A connection is also made with the recent semiclassical trajectory work of

DTIC FILE COPY

DePristo. The effects of the attractive well depth on rotational excitation and diffraction are considered.

OFFICE OF NAVAL RESEARCH

Contract N00014-81-K-0598

Task No. NR 056-766/4-21-81 (472)

Technical Report No. 10

MEAN TRAJECTORY GAUSSIAN WAVE PACKET APPROACH TO ROTATIONALLY INELASTIC MOLECULE-SURFACE DIFFRACTION

by

Bret Jackson and Horia Metiu

J. Chem. Phys., accepted (1985)

University of California
Department of Chemistry
Santa Barbara, CA 93106

Reproduction in whole or in part is permitted for any purpose of the United States Government.

This document has been approved for public release and sale; its distribution is unlimited.

Mean Trajectory Gaussian Wave Packet Approach To Rotationally Inelastic Molecule-Surface Diffraction

Bret Jackson
Department of Chemistry
University of Massachusetts
Amherst, Massachusetts 01003

and

Horia Metiu
Department of Chemistry
University of Santa Barbara
Santa Barbara, California 93106

ABSTRACT

The rotationally inelastic diffraction of H_2 from a corrugated surface is investigated using a mean trajectory model. The center of mass motion is treated using Gaussian wave packets, which propagate on a rotationally averaged potential. This trajectory in turn drives the rotational transitions. The method is non-perturbative and allows for changes in m_j, the rotational orientation, and agress well with recent close coupling calculations. A connection is also made with the recent semiclassical trajectory work of DePristo. The effects of the attractive well depth on rotational excitation and diffraction are considered.

Accesion For
NTIS CRA&I
DTIC TAB
Unannounced
Justification
By
Distribution/
Availability Codes
Dist | Avail and/or Special
A-1

I. INTRODUCTION

The interest in the collision of the lightest diatomics with surfaces has been increased by recent developments in the experimental techniques.[1-6] By using resonant multipohoton ionization, Zare[1] and his colleagues have shown that it is possible to measure the rotational distribution of H_2 molecules scattered from a surface. It is now reasonable to hope that a combination of this method with the existing time of flight measurements[4a] may permit us to study the collision of light diatomics with surfaces in much greater detail than possible until now.

Such developments will stimulate and help theoretical work that intends to establish a connection between various features of the molecule-surface potential and the observed scattering behavior, and to explain how the coupling between the center of mass motion (undergoing diffraction) and the rotational motion (undergoing rotational excitation and rotational polarization) influences the outcome of the scattering events. From a more practical point of view these phenomena may become useful surface probes since they are sensitive to both the long range (i.e., through diffraction) and the short range (i.e., through rotational depolarization and excitation) corrugation of the surface. They can also provide a good testing ground for various approximate theories of quantum dynamics and/or potentials.

In spite of the existence of many interesting theoretical papers[7-17] there is still a need for finding simple, efficient, reliable and illuminating approximate methods. The earliest work,[8a] used the coupled channel approach[8a,b] which is exact in principle, but is limited in practice by the dramatic increase in the number of channels with the kinetic energy of the incident particles. Furthermore, the complexity of the coupled channel theory for scattering by rigid surfaces is such that one cannot be optimistic about the possibility of incorporating lattice motion without using perturbation theory.

Subsequent work, searching for both computational simplicity

and an intuitive picture of collision dynamics, used a variety of approximations.

Garibaldi et. al.,[9] considered a hard, corrugated surface and used Rayleigh's approximation to deal with diffraction. This method eliminates many of the interesting features of the potential (i.e., it's "softness" and the attractive well) and assumes that the curvature and the amplitude of the corrugation are negligible with respect to the wave length associated with the center of mass motion. Furthermore it does not allow $\Delta m \neq 0$ transitions which change the projection of the angular momentum on the normal to the surface. Thus it cannot treat correctly the rotational polarization.

Several groups have used the sudden approximation,[10] which assumes that the transfer of parallel momentum takes place suddenly at the point where the incident molecule hits the surface. As a result, the variables X and Y, which give the location of the center of mass in a plane parallel to the surface, can be treated as parameters and the S-matrix $S_{jm\rightarrow j'm'}(X,Y)$ (j and m are rotational quantum numbers) can be calculated for each value of the pair (X,Y). Diffraction is then introduced in the theory by expanding $S_{jm\rightarrow j'm'}(X,Y)$ in a Fourier series in which the wave vectors are reciprocal lattice vectors; the S-matrix elements for various diffraction peaks are given by the Fourier coefficients in this series. Since the sudden approximation is an exponentiated perturbation theory, it is expected to be useful for low corrugation only.

The semi-classical perturbation theory of Miller and Smith[13] was applied to diatomic scattering from surfaces by Hubbard and Miller.[14] They used a zeroth order classical trajectory in which the periodicity of the surface is introduced in the motion parallel to the surface by adjusting the trajectory to emerge from the collision in one of the directions required by the kinematic restrictions due to parallel momentum conservation. These trajectories are used to calculate perturbatively the phase change caused by corrugation and rotational excitation. This

elegant theory provides relatively simple analytic formulae for the S-matrix and it can be modified to take into account, by perturbation theory, the effect of lattice motion.[15] The disadvantage is that one expects the theory to work only for small corrugation and when rotational excitation probabilities are small. Furthermore much of the simplicity is gained by using the potential proposed by Lennard-Jones and Devonshire[16] which does not depend on the azimuthal angle. Such a potential does not lead to correct rotational polarization.

Finally, Whaley and Light[17] have used a distorted wave approximation. The zeroth order wave function is obtained by the coupled channel method and describes the rotational excitations caused by the zero wave vector Fourier component of the potential (i.e., this is a "flat" potential obtained by averaging the true potential in the directions parallel to the surface). The other Fourier components are used to generate, by perturbation theory, diffraction and rotational polarization changes (i.e., $\Delta m \neq 0$ transitions).

In the present paper we develop a non-perturbative method based on using Gaussian wave packets (GWP) to treat the center of mass motion and the coupled channel method to deal with rotations. If the rotational excitations are forbidden throughout the collision, the theory reduces to the Drolshagen-Heller[18] theory of atom surface diffraction. If the coherence between the scattered packets is suppressed the theory reduces to an improved version of DePristo's[19] theory of rotational excitation.

The method presented here is the simplest among several versions developed by us. It keeps the lattice rigid and it uses what we call a mean trajectory approximation. The latter treats in an average way the manner in which the energy exchange between translation and rotation affects the translational motion; for this reason effects such as surface trapping induced by rotational excitation, or selective adsorption are not contained in the theory; furthermore the post-collision translational energy distribution is not given accurately. An improved method which

associates one GWP with each rotational excitation and in which the motion of the lattice is incorporated by using a Langevin equation is now being implemented.

Our hope is that if successfully completed this program will provide an efficient method which treats non-perturbatively the effects of lattice motion and corrugation to yield diffraction and rotational excitation and polarization, and can also deal with situations in which the surface is disordered. The main criticism of this method is that the use of GWP's to solve time dependent quantum problems is not a well defined approximation in which estimates for the error and the range of validity of the theory are provided. Thus confidence in the reliability of the method can be established only by extensive numerical studies.[20] However, the results of the present calculation for H_2 diffraction and rotational excitation compare well with the exact close coupled results,[8b] as well as with the other existing approximate methods[10c,17] in the parameter range where the latter are reliable.

II. THEORY

II.1 Introductory Remarks

The idea of using Gaussian wave functions to calculate time dependent quantum processes was pioneered by Heller and his coworkers.[21] The method has great flexibility in regards to the manner in which the wave function is constructed and in which it is propagated. Due to the complexity of the present problem we are using in this paper the simplest choices available. In assuming the form of the wave function we use a hybrid which treats the rotational motion by the coupled channel method and the translation of the center of mass by using a GWP. In combining the two we use the mean trajectory approximation (MTA)[22] which takes into account the effect of the rotational excitation on the motion of the center of mass in an average way. We expect MTA to be satisfactory for experiments using poor angular and time of flight resolution. An improved wave function form is provided by the multiple trajectory wave function[23] which associates a GWP (describing the translational motion) with each rotational transition.[23b]

The propagation method used here is the one we called previously[20] the simplest Heller method (SHM) which assumes that the GWP's are decoupled and stay narrow througnout the collision. Even though these conditions are not well fulfilled SHM works well for atom diffraction.[18,24] Therefore the GWP's are used here for the diffraction part only; SHM should be satisfactory in the present case as well. The propagation scheme can be improved by using the minimum error method in which the Gaussians are coupled and can have arbitrary widths.[20]

II.2 The Hamiltonian

We use a coordinate system with the X,Y axes fixed and contained in the surface plane and the Z axis pointing towards the vacuum. The nuclei of the diatomic are located at $\vec{r}_1$ and $\vec{r}_2$ and the center of mass is at $\vec{R}$. The interatomic distance is held fixed (the rigid rotor approximation) since the translational rotational and phonon energies are too small to cause vibrational

excitations. The rotational motion is described by the polar angle θ (between $\vec{r}$ and OZ) and the azymuthal angle ϕ (between the projection of $\vec{r}$ in the XOY plane and the OX axis). The Hamiltonian is

$$H = -(\hbar^2/2m)\,\nabla^2_{\vec{R}} + (2\mu|\vec{r}|^2)^{-1}\,\hat{\vec{L}}^2 + V(\vec{r}_1,\vec{r}_2) \qquad (II.1)$$

with $m = m_1+m_2$, $\vec{r} = \vec{r}_1-\vec{r}_2$, and $\mu=m_1m_2/(m_1+m_2)$. $\hat{\vec{L}}$ is the angular momentum operator. The potential is

$$V(\vec{r}_1,\vec{r}_2) = \sum_{i=1}^{2} D_i\{\exp[-2\alpha_i(z_i-z_o)]- 2\theta\exp[-\alpha_i(z_i-z_o)]\} \qquad (II.2)$$

$$-\beta_i D_i \exp[-2\alpha_i(z_i-z_o)][\cos(2\pi x_i/c_1)+\cos(2\pi y_i/c_2)].$$

Here $\vec{r}_i \equiv (x_i, y_i, z_i)$ and c_1 and c_2 are the lattice constants. When the parameter θ is zero the potential has no attractive well; θ=1 introduces a finite well depth.

II.3 The mean trajectory wave function

The mean trajectory approximation (MTA)[22] uses a wave function of the form

$$\psi(\vec{R},\theta,\phi;t) = \sum_{\alpha=1}^{N} C_\alpha G_\alpha(\vec{R};t) \sum_{i=1}^{n} c_{\alpha i}(t)\, Y_i(\theta,\phi)\exp(-i\varepsilon_i t/\hbar). \qquad (II.3)$$

The index i is a symbol for (j,m) which labels the spherical harmonics $Y_{jm}(\theta,\phi) \equiv Y_i(\theta,\phi)$. These satisfy the equation

$$(2\mu|\vec{r}|^2)^{-1}\,\hat{\vec{L}}^2\, Y_{jm}(\theta,\phi) = (j(j+1)\hbar^2/2\mu|\vec{r}|^2)Y_{jm}(\theta,\phi)=\varepsilon_j\, Y_{jm}(\theta,\phi). \qquad (II.4)$$

The Gaussian wave packet G_α is defined[21] by

$$G_\alpha(\vec{R};t) \equiv \exp\{(i/\hbar)[(\vec{R}-\vec{R}_\alpha(t))\cdot\overleftrightarrow{A}_\alpha(t)\cdot(\vec{R}-\vec{R}_\alpha(t))+\vec{P}_\alpha(t)\cdot(\vec{R}-\vec{R}_\alpha(t))]\}. \tag{II.5}$$

The matrix $\overleftrightarrow{A}_\alpha(t)$, called in what follows the width matrix of the packet α, has complex elements; it's imaginary part controls the extent of the packet's spatial localization; the real part contributes to the phase. The usual definition of a GWP includes a complex phase fator $\gamma_\alpha(t)$. We prefer to incorporate this factor into the coefficients $c_\alpha(t)$. The constants C_α are chosen so that at time t=0 the sum $\Sigma\, C_\alpha G_\alpha(\vec{R};0)$ is a plane wave in the coordinates X and Y and a normalized GWP in the direction OZ. The choice of the initial wave function is discussed in detail in Sections II.5 and III.1.A.

The present combination of a GWP representation for translation and a coupled channel representation for rotation is a new application of the Gaussian wave packet method, which we have found useful in dealing with other problems such as curve crossings[23a] or vibrational excitation by collisions.[25] There are two reasons for using such a mixed approach: the translational energy and that of the phonons are of the same order with the rotational spacing and therefore we need only few spherical harmonics to describe rotational excitation; since the representation of the rotational motion by GWP's require a large number of packets it is more practical to use spherical harmonics. On the other hand, the use of GWP's to represent the center of mass motion in a diffraction problem is more economical than the customary Fourier series expansion.[18,24]

II.4 The equations of motion and their interpretation

II.4.a. The equations of motion

To obtain the time evolution of $G_\alpha(\vec{R};t)$ and $c_\alpha(t)$ we introduce the wave function (II.3) in the time dependent Schrödinger equation and operate from the left with

$\int_0^{2\pi} d\phi \int_0^{\pi} d\theta \sin\theta\, Y_k^*(\theta,\phi)$. This leads to

$$\sum_\alpha c_{\alpha k}(t)\left[\frac{\hbar^2}{2m}\nabla^2_{\vec{R}} + i\hbar\frac{\partial}{\partial t}\right]G_\alpha(\vec{R},t) + i\hbar\sum_\alpha G_\alpha(\vec{R},t)\dot{c}_{\alpha k}(t)$$

$$= \sum_\alpha G_\alpha(\vec{R},t)\sum_i c_{\alpha i}(t)\, e^{-i(\epsilon_i-\epsilon_j)t/\hbar}\, V_{ki}(\vec{R}) \qquad \text{(II.6)}$$

where

$$V_{ki}(\vec{R}) \equiv \int_0^{2\pi} d\phi \int_0^{\pi} \sin\theta d\theta \quad Y_k^*(\theta,\phi)\, V(\vec{R},\theta,\phi)\, Y_i(\theta,\phi). \qquad \text{(II.7)}$$

To solve equation (II.6) we use a method proposed by Heller[21] which replaces the potential $V_{ki}(\vec{R})$ appearing in Eq. (II.6) with a second order Taylor expansion in powers of $\vec{R}-\vec{R}_\alpha(t)$. To obtain differential equations for $c_{i\alpha}(t)$ and the parameters appearing in the GWP's we set to zero the coefficients of various powers of $\vec{R}-\vec{R}_\alpha(t)$. These manipulations lead to

$$\dot{\overleftrightarrow{A}}_\alpha = -(2/m)\,\overleftrightarrow{A}_\alpha(t)\cdot\overleftrightarrow{A}_\alpha(t) - (1/2)\overleftrightarrow{K}\,, \qquad \text{(II.8a)}$$

$$\dot{\vec{R}}_\alpha(t) = (1/m)\vec{P}_\alpha(t) \qquad \text{(II.8b)}$$

$$\dot{\vec{P}}_\alpha(t) = -\sum_{ik}\sum c^*_{\alpha k}(t)c_{\alpha i}(t)\exp\{-i(\epsilon_i-\epsilon_k)t/\hbar\}\partial V_{ik}(\vec{R}_\alpha)/\partial\vec{R}_\alpha \qquad \text{(II.8c)}$$

and

$$i\hbar\dot{c}_{i\alpha}(t) = B_\alpha(t)c_{i\alpha}(t) + \sum_k c_{\alpha k}(t)\, V_{ik}(\vec{R}_\alpha(t))\exp\{-i(\epsilon_k-\epsilon_i)t/\hbar\}. \qquad \text{(II.8d)}$$

Here

$$B_\alpha(t) = (2m)^{-1}\vec{P}_\alpha(t)\cdot\vec{P}_\alpha(t) - \vec{P}_\alpha(t)\cdot\dot{\vec{R}}_\alpha(t) - i\hbar Tr\overleftrightarrow{A}_\alpha(t)/m, \tag{II.9a}$$

and the components of the matrix K in Eq. (II.8a) are given by

$$K_{xy}(t) = \sum_k \sum_i c_k^*(t)c_i(t)\exp\{-i(\epsilon_i-\epsilon_k)t/\hbar\}(\partial^2 V_{ij}(\vec{R}_\alpha)/\partial X_\alpha \partial Y_\alpha) \tag{II.9b}$$

with similar expressions for K_{xz}, etc.

II.4.b. The physical meaning of the packets.

The equations (II.8) permit us to calculate the properties of a wave packet, representing the center of mass motion, coupled to the rotational excitations of the diatomic. The states represented by one term in Eq (II.3) (i.e. $G_\alpha(R;t)\ \Sigma\ c_{\alpha i}(t)Y_i(\theta,\phi)\exp(-i\varepsilon_i t/\hbar)$) have physical reality only if a special kind of experiment is performed. This assumes, in a highly idealized fashion, that we have at our disposal a beam of probing particles which can interact with the incident diatomics in a volume of order 1Å^3.

Whenever a probe particle is deflected by a collision with a diatomic the plane wave representing the motion of the center of mass of the diatomic has been "reduced" to a wave packet of linear dimensions of ~ 1Å. A coincidence experiment, in which the arrival at the detector of a diatomic scattered by the surface is recorded only if this event is simultaneous with the arrival of a deflected probe particle, will measure the scattering of the wave packet prepared by the collision between the probe particle and the diatomic. Such a measurement will not detect any diffraction since the packet acts as a "corpuscule" which has lost its wave-like properties.

In the present diffraction calculation the packets are used as a labor saving device: we write the incident plane wave as a sum of packets states G_α, we propagate these packets independently by using the Eqs (II.8) and reconstruct the post-collision state by adding up coherently the scattered packets. In a diffraction experiment carried out in the absence of the probing beam the packets have no reality, in the sense that we are set up to detect only the state represented by their coherent sum

II.4.c. The effect of rotational excitation on diffraction.

To understand how diffraction is affected by the rotational degree of freedom in the present theory, it is useful to begin with the limiting case in which the initial state i=1 has j=0 and m=0 and the diatomic remains in it throughout the collision.

Thus, $c_{i\alpha}(t) = \exp\{i\gamma_\alpha(t)/\hbar\}$, and $c_{i\alpha}(t) = 0$ for $i>1$. Introducing these values of $c_{i\alpha}(t)$ in the Eqs. (II.8) leads to the following simplified equations of motion: the time evolution of the phase $\gamma_\alpha(t)$ is given by

$$-\dot{\gamma}_\alpha(t) = B_\alpha(t) + V_{11}(\vec{R}_\alpha(t)) \qquad \text{(II.10)}$$

with

$$V_{11}(\vec{R}_\alpha(t)) = \int_0^{2\pi} d\phi \int_0^{\pi} \sin\theta d\theta\, V(\vec{R},\theta,\phi)(4\pi)^{-1}; \qquad \text{(II.11)}$$

the equation of motion for momentum becomes

$$\dot{\vec{P}}_\alpha(t) = -\partial V_{11}(R_\alpha)/\partial\vec{R}_\alpha \quad , \qquad \text{(II.12)}$$

and the matrix $\overleftrightarrow{K}$ has the elements

$$K_{xy}(\vec{R}_\alpha) = \partial^2 V_{11}(\vec{R}_\alpha)/\partial X_\alpha \partial Y_\alpha \quad , \text{ etc.} \qquad \text{(II.13)}$$

These equations are identical with the GWP equations for atom diffraction in which the angle averaged diatomic - surface potential plays the role of an atomic-like potential for the center of mass.

A slightly more complex limiting case is that in which we consider two states only (e.g. i=1 is j=0, m=0 and i=2 is j=1, m=0). It is of course a very poor approximation to neglect the states j=1, m=1 and j=1, m=-1, etc., but we do this for the sake of simplicity; the insights gained in this way can be extended easily to more than two states. The equations (II.8d) can be written in the form

$$i\hbar\dot{c}_{1\alpha}(t) = H_{11}(\vec{R}_\alpha(t))c_{1\alpha}(t) + H_{12}(\vec{R}_\alpha(t))c_{2\alpha}(t) \qquad \text{(II.14)}$$

with

$$H_{11}(\vec{R}_\alpha(t)) = B_\alpha(t) + V_{11}(\vec{R}(t)) \qquad \text{(II.15)}$$

and

$$H_{12}(\vec{R}_\alpha(t)) = V_{12}(\vec{R}_\alpha(t)) \exp\{-i(\epsilon_2-\epsilon_1)t/\hbar\} \ . \qquad \text{(II.16)}$$

An equation for $\dot{c}_{2\alpha}$ can be obtained by interchanging 1 and 2 in Eq. (II.14). We can now integrate Eq. (II.14) and obtain

$$c_{i\alpha}(t) = \exp\{(i/\hbar) \int_o^t [B_\alpha(\tau) + V_{ii}(\vec{R}_\alpha(\tau))]d\tau\} \ a_{i\alpha}(t) \qquad \text{(II.17)}$$

with

$$a_{i\alpha}(t) = c_{i\alpha}(o)-(i/\hbar) \int_o^t dt' \ V_{ik}(\vec{R}_\alpha(t'))a_{k\alpha}(t') \qquad \text{(II.18)}$$
$$\cdot \exp\{-(i/\hbar) \int_o^{t'} d\tau[\epsilon_2+V_{22}(\vec{R}_\alpha(\tau))-\epsilon_1-V_{11}(\vec{R}_\alpha(\tau))]\}.$$

Using these expressions we can rewrite the final wave function Eq. (II.3) in the form

$$\psi(\vec{R},\theta,\phi;t) = \sum_{\alpha=1}^{N_\alpha} C_\alpha G_\alpha(\vec{R};t) \exp\{(i/\hbar) \int_o^t [B_\alpha(\tau)d\tau]\} \cdot \qquad \text{(II.19)}$$
$$\sum_{i=1}^{2} \exp\{(i/\hbar) \int_o^t d\tau V_{ii}(\vec{R}_\alpha(\tau))\}|a_{i\alpha}|e^{-i\mu_{i\alpha}(t)}e^{-i\epsilon_i t/\hbar}Y_i(\theta,\phi).$$

Again for the sake of simplicity we examine first the case of a rotationally selected diffraction measurement in which we record only the angular distribution of the diatomics arriving at the detector in state 1. The scattered intensity for this process is given by

$$I = \left|\int d\vec{R} e^{-i\vec{K}_f\vec{R}} \int Y_1(\theta,\phi)^* \sin\theta d\theta d\phi\ \psi(\vec{R},\theta,\phi;t)\right|^2 =$$

$$\sum_\alpha \sum_\beta C_\alpha^* C_\beta \langle\vec{K}_f|G_\beta\rangle\langle G_\alpha|\vec{K}_f\rangle |a_{1\alpha}||a_{1\beta}| e^{+i(\mu_{1\alpha}-\mu_{1\beta})}$$

$$\cdot\exp\{-(i/\hbar)\int_0^t d\tau\ [B_\alpha^* + V_{11}(\vec{R}_\alpha(t)) - B_\beta - V_{11}(\vec{R}_\beta(t))]\} \quad . \tag{II.20}$$

Since the particle starts and ends the collision in the state 1 we are considering an elastic process; however, we do not prevent as we did in the earlier discussion "virtual" rotational excitations from taking place. Since diffraction is mainly determined by the relationship between the phases of various packets appearing in the sum in Eq. (II.20) it is useful to note that there are two kinds of phases. The phase $\int d\tau[B_\alpha+V_{11}(\vec{R}_\alpha(\tau))]$ depends on how the packet G_α moves on the rotationally averaged potential $H_{11}(\vec{R}_\alpha(\tau))$. This is the phase that appears in the atom diffraction limit discussed above. The phase $\mu_{1\alpha}(t)$ appears because the diatomic undergoes "virtual" transitions 1→2 and 2→1 as it evolves from the initial state 1 to the final state 1. This phase is absent in the atom-like limit in which such virtual transitions are forbidden. The presence of $\mu_{i\alpha}$ leads to a dephasing similar to the Debye-Waller effect of the phonons: they arise because virtual transitions take place during elastic scattering. We expect this dephasing to diminish the peak intensity but not to broaden the peak since it is unlikely that the virtual excitations occurring at different places on the surface are correlated.

We can analyse in a similar manner an angular distribution measurement that records only diatomics reaching the detector in state 2. A measurement that records the diatomic regardless of its rotational state consists of a coherent superposition of the 1→1 and 1→2 processes and therefore consists of their sum and the interference between them.

While this analysis is not quantitative it does reveal the basic physical processes by which the rotational internal degrees of freedom affect diffraction. A very similar discussion could be made if we were to consider the diffraction of a diatomic which can be vibrationally excited by the collision (of course the kinetic energy would have to be rather large for this process to occur) or the diffraction of an atom (e.g., Li) which can be ionized during the collision process.

II.4.d. The rotational excitation.

The two level limiting case summarized by Eqs.(II.14-16) can also be used to discuss qualitatively the rotational excitation process. This process is driven by the time dependence of the matrix element $V_{12}(\vec{R}_\alpha(t))$ which is controlled by the time dependence of the center of mass position $\vec{R}_\alpha(t)$. This is very similar to the way in which the nuclear motion induces charge transfer in two state models.[23a,25] However, the trajectory $\vec{R}_\alpha(t)$ appearing here is not a classical trajectory but it contains some feed-back regarding the effect of the instantaneous state of rotational excitation on the center of mass motion; this is achieved through the presence of the potential $\Sigma\,\Sigma\, c^*_{i\alpha}(t)\, c_{k\alpha}(t)\, V_{ik}(\vec{R}_\alpha(t))$ in the Eqs. (II.8). Since this feature is typical of MTA we are not discussing it further and refer to our previous work regarding the use of MTA in curve crossing problems.[22a]

II.5 The construction of the initial wave function.

The construction of the initial wave function from an expression of the form (II.3) follows the work of Drolshagen and Heller[18] and Jackson and Metiu.[24] Since we intend to describe diffraction we must insure that $\psi(\vec{R},\theta,\phi;t=0)$ is a planar wave in the (X,Y) variables, (or that it represents the coherence properties of the beam used in experiments).

$$\psi(\vec{R},\theta,\phi;t=0) = G(z) \sum_{\alpha=1}^{N} \exp\{(i/\hbar)[([X-X_\alpha(0)]^2 + (Y-Y_\alpha(0))^2]A + P_x(0)(X-X_\alpha(0)) + P_y(0)(Y-Y_\alpha(0))]\} \cdot (\pi\hbar/2A)^{3/2} \qquad (II.21)$$

with

$$G(z) = \exp\{(i/\hbar)[A(Z-Z(0))^2 + P_z(0)(Z-Z(0)) + P_z(0)Z(0)]\}. \qquad (II.22)$$

The sum in Eq. (II.21) is the two dimensional expression obtained by discretizing the identity

$$\exp\{i\vec{P}\cdot\vec{R}/\hbar\} = C\int d\vec{R}_o \exp\{(i/\hbar)[(\vec{R}-\vec{R}_o)\cdot\overleftrightarrow{A}\cdot(\vec{R}-\vec{R}_o) + \vec{P}\cdot(\vec{R}-\vec{R}_o) + \vec{P}\cdot\vec{R}_o\} \tag{II.23}$$

(C is a normalization constant) in order to build a two dimension plane wave. The positions X_α, Y_α are taken on a grid covering the unit cell. $P_x(0)$ and $P_y(0)$ are the components of the mean parallel momentum of the incident planar wave. The factor $(\pi\hbar/2A)^{3/2}$ normalizes the Gaussians. The Z dependence of the wave function is given by a GWP; the manner in which this choice affects beam coherence has been discussed by Jackson and Metiu.[24] The position Z(0) is taken outside the surface-molecule interaction region. This procedure fixes the constant C_α appearing in Eq. (II.3) to

$$C_\alpha = \exp[(i/\hbar)\vec{P}_o\cdot\vec{R}_o]\ (\pi\hbar/2A)^{3/2} \quad . \tag{II.24}$$

Thus all the initial conditions for the equations of motion (II.8) are specified as long as numerical values are chosen for A. The choice of the latter is discussed in Section III.1.A.

II.6 A critical discussion of the approximation.

The theory outlined here makes three approximations: The mean trajectory approximation imposing a wave function of the form (II.3-4); it assumes that the Gaussians can be propagated independently and the potential expanded around the center (SHM); and it uses a rigid lattice. We discuss below the limitations of these assumptions, and outline our current work aimed at improving the theory.

As we have discussed in Section II.2 in the limit of elastic scattering (i.e., $|c_{\alpha 1}(t)|^2 = 1$ and $|c_{\alpha n}(t)|^2 = 0$, n = 2, ...), the present calculation is identical to that of an atom scattering by a surface. Numerical work has shown[18,24] that SHM with a wave

function of the form (II.3-4) gives a satisfactory description of the problem even though some questions remain concerning the ability to describe the coherence of the incident state.[26] The wave function (II.3-4) leaves out some important details on the description of the rotational excitation's effect on the motion of the center of mass. The rotational spacing for H_2 is of the same order of magnitude as the translational kinetic energy and the rotational excitations cause the appearance of new diffraction peaks. Their positions can be obtained from energy and parallel momentum conservation conditions. The mean trajectory approximation is not likely to give the correct intensity of these peaks. To understand why we compare the MTA wave function (II.3-4) with the multiple trajectory approximation form[23]

$$\psi(\vec{R},\theta,\phi;t) = \sum_{\alpha}\sum_{i} C_{i\alpha}G_{\alpha i}(\vec{R};t)c_{\alpha i}(t)Y_i(\theta,\phi)e^{-i\epsilon_i t/\hbar} \quad \text{(II.25)}$$

which associates one GWP with each rotational state rather than one GWP for all of them. If we consider, for simplicity, a two state problem (i.e. two rotational states Y_1 and Y_2), the collision described by the wave function (II.25) can generate two packets for each α: one, $G_{\alpha 1}$, having the same energy as the incident packet and the other, $G_{\alpha 2}$, having the incident energy minus the energy of the rotational excitation. The coherent sum $\sum_{\alpha} G_{\alpha 2}$ is used to calculate the intensity of the new, rotationally shifted diffraction peaks while $\sum_{\alpha} G_{\alpha 1}$ generates the intensity of the rotationally elastic diffraction peaks. The behavior of the single packet G_{α} used by MTA is an average of the behavior of $G_{\alpha 1}$ and $G_{\alpha 2}$.

The usefulness of MTA depends on the measurements being analyzed. If one is interested in rotational population measured with poor angular resolution MTA should be satisfactory, the averaging effect of the large detector aperture is simulated by the MTA wave function. If one is interested in detailed, highly resolved angular distributions one should use the multiple

trajectory approximation. In the same vein, detailed time of flight measurements (TOF) require the use of multiple trajectories, while MTA is satisfactory if the TOF resolution is poor.

The SHM assumptions that the Gaussians G_α can be propagated independently and that the potential can be replaced by a local quadratic expansion around the center of the packet, can both be removed. The general procedure for accomplishing this was discussed elsewhere,[20] and we hope to apply it to the present problem soon.

Finally, the thermal motion of the lattice can be incorporated into the present calculation in a manner similar to that employed in our work on diffraction[26] which included the classical motion of the lattice atom through a Langevin equation.

III. NUMERICAL RESULTS

III.1. Computational Details

The numerical calculations reported here use the wave function (II.3) with the coefficients C_α given by (II.24). The time evolution of the wave function given by the time dependence of the parameters $\overleftrightarrow{A}_\alpha(t)$, $\vec{R}_\alpha(t)$, $\vec{P}_\alpha(t)$ and $c_\alpha(t)$ is determined by solving the first order differential equations (II.8). The choice of the initial conditions for these parameters and of the molecule-surface interactions are discussed below.

III.1.A The choice of the initial wave function

The proceudre used for choosing the initial parameters in the wave function was explained in Section II.5. We give some additional details. The surface is a square lattice with the lattice constants $c_1=4A$ and $c_2=2A$. To construct the incident two dimensional plane wave (see Section II.3) we place in a plane parallel to the surface and located at a distance Z(0) a rectangle of the size of the unit cell. We divide it into N_α subcells. In the center of the Gaussian G_α we palce a subcell α. This fixes $X_\alpha(0)$, $Y_\alpha(0)$ and $Z_\alpha(0)$. We test the results and see that the results are not sensitive to these choices by increasing $Z_\alpha(0)$ and/or by increasing the number of cells.

The intial momentum $\vec{P}(0)$ was chosen so that $\vec{P}(0) = \hbar\vec{k}_o$ where $\vec{k}_o$ is the initial wave vector. The initial phase of the packet G_α is given by $\vec{R}_\alpha(0)\cdot\vec{P}(0)$ (see Eq. (II.23)).

The choice of the elements of the matrix A(0) is more difficult and involves some arbitrariness. We assume that $\overleftrightarrow{A}(0) = A\overleftrightarrow{I}$ where $\overleftrightarrow{I}$ is the unit matrix. Following Drolshagen and Heller,[18] the diagonal elements of A are chosen to give a narrow packet at the point of impact with the surface. The justification for this procedure is that the propagation scheme works best for narrow Gaussians, therefore we can use the flexibility in chosing the magnitude of A to make the packet narrow at the most important point along the trajectory, i.e., the point of impact. An inexpensive way of implementing this idea is to use for A(t) the free space formula and determine A(0

to give at the time of impact t_c the desired values for $A(t_c)$. In our previous work[22] we have shown that the interaction affects strongly the magnitudes of $ImA_{xx}(t)$, $ImA_{yy}(t)$, and $ImA_{zz}(t)$. Also, packets which correspond to particles of very small mass (e.g., He, H_2) broaden very quickly. As a result, the GWP's are much broader during the interaction than would be desirable. Thus we are not achieving the objective that was used to justify the procedure. Nevertheless, the procedure works in the sense that predictions made for atom diffraction agree with the exact calculations, and the results are stable with respect to small varitions in the value of A(0). Perhaps this happens because diffraction is dominated by the phases of the GWP's and in SHM the phases are essentially given by the classical action. Thus the SHM results have, roughly, the same accuracy as those of the semi-classical diffraction theory. Since the latter works reasonably well so will SHM, as long as the contributions to the S-matrix due to the widths of the packets are less important than those due to their phases. If this is the case the results are not sensitive to small changes in $A_\alpha(t)$ caused by changes in the choice of the initial value A. However other applicatons[20] of the GWP method indicate that a proper choice of the initial parameters (by varying the parameters in the GWP expression for the wave function to get the best fit of the initial condition) is sometimes very important. Therefore we regard the freedom in the choice of A as an unsatisfactory feature of the present theory.

III.1.B The computed quantities

We propagate the packets for a time τ sufficient to allow them to emerge from the interaction region. The observables computed here become independent of the time when the packets are no longer interacting with the surface. The S-matrix for a H_2molecule emerging in the final state

$$q_z^{1/2}\exp(i\vec{q}\cdot\vec{R})\ Y_i(\theta,\phi) \qquad \text{(III.1)}$$

is

$$S^{(i)}_{nm} = ((q_z)^i_{nm})^{1/2} \sum_{\alpha=1}^{N} \int d\vec{R}\, \exp(-i\vec{q}^{\,i}_{nm}\cdot\vec{R})\, G_\alpha(\vec{R};\tau)\, C_\alpha c_{\alpha i}(\tau) \; ; \tag{III.2}$$

the probability of reaching the specified final state is $P^i_{nm} = |S^i_{nm}|^2$.

The final momenta must satisfy parallel momentum and energy conservation and are constrained to take the values

$$(q_x)^i_{nm} = k_{ox} + 2\pi n/c_1 \tag{III.3a}$$

$$(q_y)^i_{nm} = k_{oy} + 2\pi m/c_2 \tag{III.3b}$$

and

$$(q_z)^i_{nm} = (\vec{k}_o^2 - [(q_x)^i_{nm}]^2 - [(q_y)^i_{nm}]^2 - \frac{2m\epsilon_i}{\hbar^2})^{1/2} \; . \tag{III.3c}$$

Here $\vec{k}_o = \vec{P}_o/\hbar$ and $\vec{P}_o$ is the initial mean momentum of the packets. As usual the integers (n,m) label the diffraction peaks.

The above equations refer to scattering from one unit cell. The S-matrix for the whole surface can be obtained by adding the S-matrices for each cell weighted with the the proper exponential factors requied by the two dimensional peridocity. When this is squared it leads to δ functions which give (III.3a) and (III.3b).

III.2 Numerical results for a potential without an attractive well.

In order to compare our results with other calculations we use the potential given by Eq. (II.2) with θ=0 and the parameter set 1 given in Table I. We denote this potential V_1. By taking θ=0, we suppress the molecule-surface attraction. The incident H_2 molecules move in a direction perpendicular to the surface, have a kinetic energy of 0.1 eV and are in the state j=0, m=0 corresponding to para-hydrogen. We denote this calculation S_1.

The results of our calculations, together with those obtained by multichannel distorted wave (MDW)[17], the diffractive sudden rotational close coupling (DSCCR)[10c], and the exact close coupled (CC) methods,[8b] are given in Table II.

The agreement is rather good, even over ten orders of magnitude, considering that the mean trajectory method treats the translation in an average manner. One should note that both MDW and DSCCR are valid for small β and little off-specular scattering. Thus, our results should be similar to theirs for low β systems such as metal surfaces. When there is strong off specular scattering, which is the case for experimental systems such as H_2/LiF or D_2/NaF, the other methods should break down. Our method should correctly predict the rotational transitions in this limit.

Note that one disagreement between the present theory, the MDW calculation,and the DSCCR results is for the specular peak. This is not surprising because in the MDW approach the zeroth order state is taken to correspond to β=0 which leads only to specular scattering and Δm_j=0. First order perturbation theory is then used to compute all off specular scattering. As is well known for all first order theories, the zeroth order state is unchanged by the perturbations, and the total probability is not normalized. The problem then, is that one can not calculate the effects of having a finite corrugation on the rotation-diffraction probabilities of the specular peak, which is the only easily observable peak for the low β systems where such approaches are valid.

Thus, we see discrepancies between the MDW and exact CC results at larger B's for the specular peak. The DSCCR probabilities are very close to the exact values, while the mean trajectory results are reasonable, but not quite as good. The three approximate methods show roughly the same level of accuracy for the off specular rotationally elastic probabilities, when compared with the exact results. However, the mean trajectory method is much more accurate than either the MDW or DSCCR calculations for off specular scattering where $\Delta mj \neq 0$, for all values of β tested. For the (0,1) peak, the MDW and DSCCR results are off by a factor of 2 or more, while the mean trajectory method gives values reasonably close to the exact CC results. For the

"more sudden" (1,0) diffraction state, this difference is not very large. For the off specular $|0,0\rangle \rightarrow |2,0\rangle$ transition, the mean trajectory approach is not quite as accurate as the MDW and DSCCR for the (1,0) peak, although all are fairly close to the exact results. The mean trajectory results are much better than both MDW and DSCCR for the transition $|0,0\rangle \rightarrow (0,1)|2,0\rangle$.

Thus, the mean trajectory method is a viable approximate approach to the rotationally inelastic diffraction problem. Not only does it require a small fraction of the computer time needed by CC, MDW, and DSCCR calculations, but it is easily extended to disordered[18] or finite temperature systems,[26] or high energy systems involving a great many diffraction states. A more detailed comparison of the MDW, DSCCR, and CC methods can be found in reference 8b.

III.3 The probability of rotational excitations: a comparison with DePristo's results.

Recently DePristo[19] carried out a mean trajectory calculation of the rotational excitation caused by collisions with a surface. He used the wave function

$$\psi(\theta,\phi;t) = \sum_i c_i(t)\, Y_i(\theta,\phi) e^{-\epsilon_i t/\hbar} \qquad \text{(III.4a)}$$

with the amplitudes given by

$$i\hbar \dot{c}_i(t) = \sum_j \cdot H_{ij}(R(t))\, c_j\, e^{-(\epsilon_j-\epsilon_i)t/\hbar} \qquad \text{(III.4b)}$$

and

$$H_{ij}(R(t)) = \int_0^{\pi} \sin\theta d\theta \int_0^{2\pi} d\phi\; Y_i(\theta,\phi) V(\theta,\phi;\vec{R}(t))\; Y_j(\theta,\phi). \qquad \text{(III.4c)}$$

The center of mass motion is given by

$$m\ddot{\vec{R}}(t) = -\frac{\partial}{\partial \vec{R}(t)} \sum_i \sum_j c_i^* c_j H_{ij}(R(t)) \; . \qquad \text{(III.4d)}$$

The above equations are a limiting case of GWP-MTA obtained by replacing $c_\alpha G_\alpha(\vec{R};t)$ with 1 in Eq. (II.3) and making $B_\alpha(t)=0$ in (II.9a). A dramatic effect of the replacement $C_\alpha G_\alpha(\vec{R};t)$ with 1 is that the interference between the trajectories is lost, therefore the theory is unable to give diffraction. For heavy diatomics this is not an important error but for such cases the rotational spacing is very small and the rotational quantum effects are also negligible; therefore a fully classical calculation should be adequate. For those cases in which the rotational motion needs to be treated quantum mechanically the diffraction effects are likely to be important and we must understand how they influence the angular dependence of the rotational excitation probabilities.

DePristo's calculation assumes that this influence is negligible.

To answer such questions we compare a GWP-MTA calculation with an "incoherent GWP-MTA", that is with a calculation in which the probability P_{jm} that the particle emerges in the state j,m is given by

$$P_{jm}^{in} = \int_0^{\pi} \sin\theta d\theta \int_0^{2\pi} d\phi \sum_{\alpha} |S_{\infty \to jm}^{(\alpha)}(\theta,\phi)|^2 \qquad \text{(III.5)}$$

instead of

$$P_{jm}^{coh} = \int_0^{\pi} \sin\theta d\theta \int_0^{2\pi} d\phi \sum_{\alpha} \sum_{\beta} [S_{\infty \to jm}^{(\alpha)}(\theta,\phi)]^* [S_{\infty \to jm}^{(\beta)}(\theta,\phi)] \qquad \text{(III.6)}$$

Here $S_{\infty \to jm}(\theta,\phi)$ is the S-matrix for the transition (j=0, m=0) → (j,m) at the angles θ,ϕ, for the packet $G^{(\alpha)}$. The major approximation made by DePristo is, in essence, the replacement of (III.6) by (III.5).

The results obtained with the full GWP-MTA summed over diffraction peaks (equivalent to Eq. (III.6) and with its "incoherent" version (i.e., Eq. (III.5)) are shown in Table III. We find that the rotational excitation probabilities given by the incoherent expression, are systematically larger than those given by the coherent one. However, the errors are not very large and therefore we feel that the present calculation justifies the use of DePristo's method for light scatterers, when a qualitative analysis in intended.

III.4 The effect of an attractive well

The recent calculations[8b,10c,17] of coupled rotational excitations and diffraction with which we compare our results are confined to purely repulsive potentials. The absence of an attractive well simplifies the theory since it eliminates selective adsorption and rotationally mediated selective adsorption. From an experimental point of view this elimination is unfortunate since such resonances are very common.[2]

While the GWP-MTA theory presented here is not designed to give bound state resonances it can be used to examine the effect

of molecule-surface attraction on diffraction and rotational excitation. In particular it can examine whether there is any truth to the notion that the effect of an attractive well is roughly equivalent to a change in the normal part of incident kinetic energy by an amount equal to the well depth. We find that this is not the case.

Our first calculation with an attractive well uses Eq. (II.2) with the parameter set 2, β=.05 and Θ=1. We denote this potential V_2 and the calculation of scattering by it of a normal beam with the incident kinetic energy ϵ_o=0.1 eV is denoted C_2. We have chosen Z_o=1.8841Å and D=.02 eV so that we obtain a well depth of 0.02 eV, and the potential V_2 reduces to the potential V_1 (used in Section III.2) when we take Θ=0. The results of the calculation C_2 are shown in Table IV. When we compare them to those of C_1 (see Table II) we find substantial differences. Going from V_1 to V_2 lowers the intensity of the rotationally elastic specular peak and increases the intensity of the diffracted beams. The probability of the rotational excitation $|0,0\rangle \rightarrow |2,0\rangle$ in the specular peak goes down when the well is turned on.

We can ask whether the scattering of a 0.1 eV beam from the potential V_2, having a 0.02 eV well is equivalent to scattering from the potential V_1 with an incident kinetic energy of 0.1 + 0.02 eV. To answer the question we compare the probabilities describing the latter process (Table V) to those of the former, given in Table IV. Clearly the results are not similar. Nor are the trends in going from the calculation C_1 to C_2 similar to those seen when going from C_1 to a kinetic energy of 0.12 eV on the potential V_1.

Since the change from V_1 to V_2 not only adds an attractive well but also changes the slope of the repulsive wall and its effective corrugation, we have designed a new potential V_3 with the parameter set 3 (Table I), β=.022, and Θ=1. V_3 has a well of depth 0.02 eV and the same corrugation amplitude and repulsive force (for both ϵ = 0.1 eV and ϵ = 0.12 eV)as the potential V_1,

with β=.05. The calculation denoted C_3 gives probabilities (Table VI) for scattering with ϵ = 0.1 eV and from the potential V_3. They are still rather different from those obtained for scattering by the purely repulsive potential V_1 at the kinetic energy 0.12 eV.

It seems that for the situations presented here the presence of an attractive well has a significant influence on scattering probabilities, which cannot be predicted by assuming that the well merely changes the incident kinetic energy.

Aknowledgements: This work was supported by the National Science Foundation (CHE82-06130) and in part by the Office of Naval Research. One of us (HM) is grateful to Professor W.H. Miller for useful discussions.

REFERENCES

1. (a)E.E. Marinero, C.T. Rettner, R.N. Zare, Phys. Rev. Lett., 48, 1323 (1982); E.E. Marinero, R. Vasudev and R.N. Zare, J. Chem. Phys., 78, 692(1983); S.L. Anderson, G.D. Kubiak and R.N. Zare, Chem. Phys. Lett., 105, 22(1984). (b) G.D. Kubiak, G.O. Sitz and R.N. Zare, J. Vac. Sci. Tech. (in press); J. Chem. Phys., 81, 6397 (1984).
2. J.P. Cowin, C.F. Yu, S.J. Sibener, and L. Wharton, J. Chem. Phys., 79, 3537 (1983); C.F. Yu, K.B. Whaley, C.S. Hogg and S.J. Sibener, Phys. Rev. Lett., 51, 2210(1983); C.F. Yu, C.S. Hogg, J.P. Cowin, K.B. Whaley, J.C. Light and S.J. Sibener, Israel J. Chem., 22, 305(1982); J.P. Cowin, C.F. Yu, S.J. Sibener, C.S. Hogg and L. Wharton, in "Many Body Phenomena at Surfaces," D. Langreth and H. Suhl eds. (Academic Press, 1984).
3. A.C. Luntz, A. W. Kleyn and D.J. Auerbach, Phys. Rev., B25, 4273 (1982); A.W. Kleyn, A.C. Luntz and D.J. Auerbach, Surf. Sci., 117, 33(1982).
4. (a) G. Brosdeylins and J.P. Toennies, Surf. Sci., 126, 647(1983); W. Allison and B. Feuerbacher, Phys. Rev. Lett., 45, 2040(1980); (b) G. Boato, P. Cantini and C. Mattera, J. Chem. Phys., 65, 544(1976); R.G. Rowe and G. Ehrlich, J. Chem. Phys., 63, 4648(1975).
5. J.M. Horne, S.C. Yerkes, and D.R. Miller, Surf. Sci., 93, 47(1980).
6. J.W. Hepburn, F.J. Northrup, G.L. Ogram, J.C. Polanyi and J.M. Williamson, Chem. Phys. Lett., 85, 127(1982); G.M. McClelland, G.D. Kubiak, H.G. Rennagel, and R.N. Zare, Phys. Rev. Lett., 46, 831(1981); F. Frentel, J. Hager, W. Krieger, H. Walther, C.T. Cambell, G. Ertl, H. Kuipers and J. Senger, Phys. Rev. Lett., 46, 152(1981).
7. For a recent review, see D.J. Kouri and R.B. Gerber, Israel J. Chem., 22, 321(1982).
8. (a) G. Wolken, J. Chem. Phys., 59, 1159(1973); Chem. Phys.

Lett., 21, 373(1973); J. Chem. Phys., 62, 2730(1975); (b) J.V. Lill and D.J. Kouri, Chem. Phys. Lett. 112, 249(1984).

9. V. Garibaldi, A.C. Levi, R. Spadacini and G. E. Tommei, Surf. Sci., 55, 40(1976).

10. (a) R.B. Gerber, A.T. Yinnon, Y. Shinioni, and D.J. Kouri, J. Chem. Phys., 73, 4397(1980); R.B. Gerber, A.T. Yinnon, J.N. Murrell, Chem. Phys., 31, 1(1978); D.E. Fitz, A.O. Bawagan, L.H. Beard, D.J. Kouri, and R.B. Gerber, Chem. Phys. Lett., 80, 537(1981); D.E. Fitz, L.H. Beard, and D.J. Kouri, Chem. Phys., 59, 257(1981); R.B. Gerber, L.H. Beard and D.J. Kouri, J. Chem. Phys., 74, 4708(1981); (b) J.E. Adams, Surf. Sci., 97, 43(1980); (c) T.R. Proctor, D.J. Kouri and R.B. Gerber, J. Chem. Phys., 80, 3845(1984).

11. R. Schinke, Chem. Phys. Lett., 87, 438(1982); Surf. Sci., 127, 283(1983).

12. C.J. Ray and J.M. Bowman, J. Chem. Phys., 66, 1122(1977); J.M. Bowman and S.C. Park, J. Chem. Phys., 74, 5411(1982); J. Chem. Phys., 79, 3172(1983); S.C. Park and J.M. Bowman, J.Chem. Phys., 80, 2183(1984).

13. W.H. Miller and F.T. Smith, Phys. Rev. A17, 17(1978).

14. L.M. Hubbard and W.H. Miller, J. Chem. Phys., 78, 1801 (1983).

15. L.M. Hubbard and W.H. Miller, J. Chem. Phys. 80, 5827(1984).

16. J.E. Lennard-Jones and A.F. Devonshire, Proc. R.Soc. London Ser. A 158, 242(1937).

17. K.B. Whaley and J.C. Light, J. Chem. Phys., 81, 33334(1984).

18. G. Drolshagen and E. Heller, J. Chem. Phys., 79, 2072(1983); Surf. Sci., 139, 260(1984).

19. A.M. Richard and A.E. DePristo, Surf. Sci., 134, 338(1983); A.E. DePristo, Surf. Sci., 137, 138(1984).

20. S. Sawada, R. Heather, B. Jackson and H. Metiu, J. Chem. Phys. (in press).

21. a) E.J. Heller, J. Chem. Phys., 62, 1544 (1975); b) ibid.,

65, 4979 (1976); c) K.C. Kulander and E.J. Heller, ibid., 69, 2439(1978); d)E.J. Heller, ibid., 68, 2066, 3891(1978); e) S.Y. Lee and E.J. Heller, ibid., 71, 4777 (1978); f) M.J. David and E.J. Heller, ibid., 71, 3383(1979); g) R.B. Brown and E.J. Heller, ibid., 75, 186(1981); h) S.Y. Lee and E.J. Heller, ibid., 76, 3035(1982); i) D.J. Tannor and E.J. Heller, ibid., 77, 202 (1982); j) E.J. Heller, R.L. Sundberg, and D. Tannor, ibid., 86, 1822 (1982); k) N. DeLeon and E.J. Heller, ibid., 78, 4005 (1983).

22. (a) S. Sawada, A. Nitzan and H. Metiu, Phys. Rev. B (in press); S. Sawada and H. Metiu, Phys. Rev. B (submitted); (b) M.H. Mittelman, Phys. Rev. 122, 499(1961); G. D.Billig, Chem. Phys. Lett., 30, 391 (1975); Chem. Phys. 70, 223(1982); J.B. Delos, W. B. Thorson and S.K. Knudson, Phys. Rev. A6, 709(1972); J.T. Muckerman, I. Rusinek, R.E. Roberts and M. Alexander, J. Chem. Phys., 65, 2416(1976); S.D. Augustin and H. Rabitz, J. Chem. Phys., 69, 4195(1978); D. Kumanoto and R. Silbey, J. Chem. Phys., 75, 5164 (1981); D.J. Diestler, J. Chem. Phys., 78, 2240(1983).

23. (a) S. Sawada and H. Metiu, J. Chem. Phys.; b) B. Jackson and H. Metiu (to be published).

24. B. Jackson and H. Metiu, J. Chem. Phys. 82, 5707(1985).

25. R. Heather and H. Metiu (in preparation).

26. B. Jackson and H. Metiu, J. Chem. Phys. 83, 1952 (1985).

Table I. The values of some of the parameters appearing in the potential (Eq. II.2). The remaining parameters are specified in the text.

Parameter Set	1	2	3
α (A^{-1})	1.83315	1.83315	1.17
Z_o (A)	0.0 A	1.8841	2.5
D (eV)	20.0	0.02	0.02
c_1 (A)	4.0	4.0	4.0
c_2 (A)	2.0	2.0	2.0

Table II. Transition probabilities $|j,m\rangle = |0,0\rangle \rightarrow G'|j',m'\rangle$ for H_2 on a rectangular lattice at normal incidence. Results are for the Multichannel Distorted Wave[17] (MDW), close coupled[66] (cc), mean trajectory (this work), and diffraction sudden rotation close coupled[10c] theories respectively. The calculation was performed for parameter set 1 of Table I for 3 values of the corrugation parameter β.

		$\|j'm'\rangle$			
G'	β	$\|0,0\rangle$	$\|2,2\rangle$	$\|2,1\rangle$	$\|2,0\rangle$
		CC			
	.005	.904	.832(-10)	0	.957(-1)
(0,0)	.05	.860	.814(-6)	0	.920(-1)
	.1	.737	.122(-4)	0	.813(-1)
	.005	.140(-3)	.431(-7)	.123(-6)	.111(-4)
(1,0)	.05	.136(-1)	.464(-5)	.121(-4)	.109(-2)
	.1	.500(-1)	.231(-4)	.456(-4)	.406(-2)
	.005	.826(-4)	.335(-6)	.194(-6)	.640(-5)
(0,1)	.05	.800(-2)	.327(-4)	.189(-4)	.624(-3)
	.1	.290(-1)	.121(-3)	.704(-4)	.230(-2)
		MEAN TRAJECTORY			
	.005	.917	.854(-10)	~.3(-18)	.825(-1)
(0,0)	.05	.877	.997(-6)	~.3(-16)	.792(-1)
	.1	.759	.155(-4)	~.2(-16)	.697(-1)
	.005	.146(-3)	.412(-7)	.115(-6)	.984(-5)
(1,0)	.05	.136(-1)	.446(-5)	.112(-4)	.930(-3)
	.1	.501(-1)	.225(-4)	.416(-4)	.349(-2)
	.005	.744(-4)	.370(-6)	.243(-6)	.522(-5)
(0,1)	.05	.675(-2)	.362(-4)	.239(-4)	.526(-3)
	.1	.246(-1)	.135(-3)	.911(-4)	.195(-2)

Table II. continued

G'	β	|0,0>	|2,2>	|2,1>	|2,0>
			MDW		
	.005	.893	0	0	.106
(0,0)	.05	.893	0	0	.106
	.1	.893	0	0	.106
	.005	.138(-3)	.467(-7)	.138(-6)	.125(-4)
(1,0)	.05	.138(-1)	.467(-5)	.138(-4)	.125(-2)
	.1	.553(-1)	.187(-4)	.552(-4)	.500(-2)
	.005	.898(-4)	.634(-6)	.465(-6)	.932(-5)
(0,1)	.05	.898(-2)	.634(-4)	.465(-4)	.932(-3)
	.1	.359(-1)	.254(-3)	.186(-3)	.373(-2)
			DSCCR		
	.005	.905	.843(-10)	0	.948(-1)
(0,0)	.05	.859	.822(-6)	0	.905(-1)
	.1	.441	.103(-4)	0	.157(-2)
	.005	.142(-3)	.506(-7)	.154(-6)	.117(-4)
(1,0)	.05	.137(-1)	.549(-5)	.149(-4)	.113(-2)
	.1	.130	.156(-4)	.433(-5)	.329(-3)
	.005	.925(-4)	.696(-6)	.519(-6)	.867(-5)
(0,1)	.05	.890(-2)	.672(-4)	.503(-4)	.838(-3)
	.1	.814(-1)	.507(-4)	.147(-4)	.233(-3)

Table III. Comparison of incoherent (P^{in}_{jm}; Eq. III.5) and coherent diffraction summed (Σ) mean trajectory transition probabilities $|0,0\rangle \rightarrow |j',m'\rangle$ for the system described in Table II.

	β	$\|0,0\rangle$	$\|2,2\rangle$	$\|2,1\rangle$	$\|2,0\rangle$
P^{in}_{jm}	.005	.872	.241(-5)	.169(-5)	.126
	.05	.872	.240(-3)	.170(-3)	.127
	.1	.871	.969(-3)	.698(-3)	.125
Σ	.005	.917	.823(-6)	.716(-6)	.825(-1)
	.05	.918	.823(-4)	.702(-4)	.821(-1)
	.1	.908	.331(-3)	.265(-3)	.806(-1)

Table IV. Transition probabilities $|0,0\rangle \rightarrow (n,m)|j'm'\rangle$ for an incident beam of .1 eV H_2 molecules, using parameter set 2 with $\theta = 1$, and $\beta = .05$. Also included are the incoherent (P^{in}_{jm}) and diffraction summed results (Σ).

	$\|0,0\rangle$	$\|2,0\rangle$	$\|2,1\rangle$	$\|2,2\rangle$
(0,0)	.730	.237(-1)	$\sim 10^{-16}$	.282(-4)
(±1,0)	.676(-1)	.197(-2)	.446(-5)	.448(-4)
(0,±1)	.400(-1)	.150(-2)	.127(-4)	.216(-3)
(±1,±1)	.333(-2)	.110(-3)	.147(-5)	.125(-4)
(±2,0)	.121(-2)	.288(-4)	.444(-6)	.225(-5)
(0,±2)	.200(-3)	.674(-5)	.872(-6)	.320(-5)
P^{in}_{jm}	.951	.0448	.108(-3)	.152(-2)
Σ	.967	.312(-1)	.428(-4)	.611(-3)

Table V. Transition probabilities $|0,0\rangle \rightarrow (n,m)|j',m'\rangle$, and incoherent and diffractive summed results for an incident beam of .12 eV H_2 molecules, using parameter set 1, with $\theta=0$ and $\beta=.05$.

	$\|0,0\rangle$	$\|20\rangle$	$\|21\rangle$	$\|22\rangle$
(0,0)	.843	.102	$\sim 10^{-15}$	.171(-5)
(±1,0)	.158(-1)	.158(-2)	.147(-4)	.710(-5)
(0,±1)	.830(-2)	.987(-3)	.331(-4)	.591(-4)
(±1,±1)	.104(-3)	.101(-4)	$<10^{-6}$	$<10^{-6}$
P_{jm}^{in}	.850	.148	.198(-3)	.330(-3)
Σ	.892	.107	.956(-4)	.134(-3)

Table VI. Transaction probabilities $|0,0\rangle \rightarrow (n,m)|j',m'\rangle$, and incoherent and diffractive summed results for an incident beam of .1 eV H_2 molecules, using parameter set 3, with ϵ=1 and β =.022.

	$\|0,0\rangle$	$\|2,0\rangle$	$\|2,1\rangle$	$\|2,2\rangle$
(0,0)	.766	.128	$\sim 10^{-16}$	.831(-5)
(±1,0)	.311(-1)	.459(-2)	.626(-5)	.130(-4)
(0,±1)	.137(-1)	.267(-2)	.150(-4)	.813(-4)
(±1,±1)	.449(-3)	.778(-4)	.563(-6)	.189(-5)
P^{in}_{jm}	.799	.198	.9(-4)	.496(-3)
Σ	.857	.143	.448(-4)	.204(-3)

END

FILMED

5-86

DTIC